Pramana – J. Phys. (2021) 95:94
https://doi.org/10.1007/s12043-021-02126-9

Emergence of quantum phases for the interacting helical liquid of topological quantum matter

RANJITH R KUMAR[1,2], S RAHUL[1,2], SURYA NARAYAN[3] and SUJIT SARKAR[1,*]

[1]Theoretical Sciences Division, Poornaprajna Institute of Scientific Research, Bidalur, Bengaluru 562 164, India
[2]Manipal Academy of Higher Education, Madhava Nagar, Manipal 576 104, India
[3]Raman Research Institute, C.V. Raman Avenue, 5th Cross, Sadashivanagar, Bengaluru 560 080, India
[*]Corresponding author. E-mail: sujit.tifr@gmail.com

MS received 4 November 2020; revised 5 February 2021; accepted 9 February 2021

Abstract. Emergence of different interesting and insightful phenomena in different length scales is the heart of quantum many-body system. We present emergence of quantum phases for the interacting helical liquid of topological quantum matter. We also observe that Luttinger liquid parameter plays a significant role to determine different quantum phases. We use three sets of renormalisation group (RG) equations to solve emergent quantum phases for our model Hamiltonian system. Two of them are the quantum Berezinskii–Kosterlitz–Thouless (BKT) equations. We show explicitly from the study of length scale-dependent emergent physics that there is no evidence of Majorana–Ising transition for the two sets of quantum BKT equations, i.e., the system is either in the topological superconducting phase or in the Ising phase. The whole set of RG equation shows the evidence of length scale-dependent Majorana–Ising transition. Emergence of length scale-dependent quantum phases can be observed in topological materials which exhibit fundamentally new physical phenomena with potential applications for novel devices and quantum information technology.

Keywords. Emergent physics; topological quantum phase transition; Berezinskii–Kosterlitz–Thouless transition; Majorana–Ising transition.

PACS Nos 64.60.ae; 73.20.At; 73.43.−f

1. Introduction

In quantum many-body physics, emergent phenomena are an essential aspect. In this view, fundamentally new types of phenomena emerge within the complex assemblies of particles which cannot be anticipated from *a priori* knowledge of the microscopic laws of nature [1]. One can raise the question at the fundamental level: what emergent principles and laws develop as we proceed from the microscopic scale to the macroscale scale? P W Anderson was the first to introduce the concept of 'emergent phenomena' into physics [2,3]. He has introduced this concept in "More is different", where he has explained the philosophy of emergence. The behaviour of large and complex aggregation of elementary particles cannot be comprehended in terms of simple extrapolation properties of a few particles. Instead, at each level of complexity, entirely new properties appear and the understanding of the new behaviour trigger a new front of research area. One can understand the physics and philosophy of emergence phenomena, from the following example given by Anderson in [2]. When one consider similar atoms of niobium and gold, at the angstrom level (up to 30 nm) there is no difference between them, but in the macroscopic level one is an insulator and other is a superconductor. But when we consider the large length scale, everything changes. Gold behaves as a very good metal. In niobium beyond 30 nm the electrons pair up into Cooper pairs. As one reaches the micron scale, these pairs congregate by the billion into a pair of condensate, transforming the crystal into an entirely new metallic state which is type-II superconductor. This emergent properties in different length scale is the motivation for the present study. We analyse how the different quantum phases appear in different length scales for interacting helical liquid of topological quantum matter. In the last decade, since the ground-breaking discovery of topological insulators (TIs) induced by strong spin–orbit interactions,

Published online: 31 May 2021

tremendous progress has been made in our understanding of topological states of quantum matter [4,5]. Meanwhile, topological materials have become the focus of intense research in recent years, because they exhibit fundamentally new physical phenomena with potential applications for novel devices and quantum information technology [6,7].

The best known example of a topological phase is the integer quantum Hall state, in which protected chiral edge states give rise to a quantised transverse Hall conductivity [8]. These edge states arise due to a non-trivial wave function topology, that can be measured in terms of a quantised topological invariant, i.e., the Chern or TKNN number [9]. Topological phase induced by the spin–orbit coupling (preserving time-reversal symmetry) can lead to the quantum spin-Hall state [10–12]. In the absence of external magnetic field, the edge of quantum spin-Hall state support electrons with opposite spin angular momentum moving in opposite directions. This one-dimensional conducting edge is referred to as 'helical liquid' [13]. The physics of interacting helical liquid is one of the recent area of interest in topological quantum matter [14–16].

Here we consider an interacting helical liquid system at the edge as our model Hamiltonian. The quantum spin-Hall systems are associated with the helical liquid system which describes the connection between spin and momentum. The left movers in the edge of quantum spin-Hall systems are associated with down-spin and right movers with up-spin. The helical liquid system possesses gapless excitation at the edge and this results in the appearance of Majorana particles at both ends of the system [16].

Motivation of this study: The physics of topological state of quantum matter is the second revolution of quantum mechanics [17]. This important concept and new important results with high impact creates interest not only in the general public for different branches of physics but also for other branches of science (mathematics, chemistry, biology, engineering and also the philosophy of science). Our fundamental motivation is to study the emergence of quantum phases in different length scales for the topological quantum matter.

The mathematical structure and results of the renormalisation group (RG) theory are the most significant conceptual advancements in quantum field theory in the last several decades in both high-energy and condensed matter physics [18–21]. RG theory is a formalism that relates the physics at different length scales in condensed matter physics and the physics at different energy scales in high-energy physics. In the present study we derive and solve three sets of RG equations, for interacting helical liquid system. Two of them are the quantum Berezinskii–Kosterlitz–Thouless (BKT) transitions [22–24] and the third one is entirely different from the quantum BKT transition.

In helical Luttinger liquid (LL), one can observe the Dirac point due to the crossing of the left and right moving branches, also electrons with opposite spins move in opposite directions. We consider this physics for the present model Hamiltonian system where the Luttinger parameter (K) determines the nature of interaction. $K < 1$ and $K > 1$ characterise the repulsive and attractive interactions respectively, whereas $K = 1$ characterises the non-interacting situation. The present study shows the importance of K in the emergence of different quantum phases and the transition among them.

Sarkar [16] has already done the length scale-dependent study of the couplings for the interacting helical liquid but the emergent physics at different length scale has not been explored in detail for the whole sets of RG equations and also in that study the author has not derived the quantum BKT equations and the results based on these equations.

In the present study, we have also done the emergent physics from the study of quantum BKT equations for both couplings and finally we make a comparison on how the emergent behaviour of different quantum phases agree and differ from the study of three sets of RG equations.

2. Model Hamiltonian

We consider the one-dimensional interacting helical liquid system at the edge of a topological insulator as our model system [25]. These edge states are protected by the symmetries [26]. In the edge states of the helical liquid, spin and momentum are connected as the right movers are associated with spin-up and left movers are associated with spin-down. One can write the total fermionic field of the system as

$$\psi(x) = \mathrm{e}^{ik_{\mathrm{F}}x}\psi_{R\uparrow} + \mathrm{e}^{-ik_{\mathrm{F}}x}\psi_{L\downarrow},$$

where $\psi_{R\uparrow}$ and $\psi_{L\downarrow}$ are the field operators corresponding to the right moving (spin-up) and left moving (spin-down) electrons at the upper and lower edges of the topological insulators [13,15,16,27]. For the low-energy collective excitation in one-dimensional system, one can write the Hamiltonian as

$$H_0 = \int \frac{\mathrm{d}k}{2\pi} v_{\mathrm{F}}[(\psi_{R\uparrow}{}^{\dagger}(i\partial_x)\psi_{R\uparrow} - \psi_{L\downarrow}{}^{\dagger}(i\partial_x)\psi_{L\downarrow}) + (\psi_{R\downarrow}{}^{\dagger}(i\partial_x)\psi_{R\downarrow} - \psi_{L\uparrow}{}^{\dagger}(i\partial_x)\psi_{L\uparrow})], \quad (1)$$

where the terms in parentheses represent Kramer's pair at the two edges of the system.

The authors of refs [15,16] have mapped this Hamiltonian, with forward and umklapp interactions and in the proximity of s-wave superconductor (Δ) and the magnetic field (B), to the XYZ spin-chain model (up to a constant), i.e., $H_{XYZ} = \sum_i H_i$, where

$$H_i = \sum_{\alpha} J_\alpha {S_i}^\alpha {S_{i+1}}^\alpha - [\mu + B(-1)^i]{S_i}^z. \tag{2}$$

From the bosonisation procedure, fermionic field of 1D quantum many-body system can be expressed as

$$\psi_{R/L,\uparrow}(x) = \frac{1}{2\pi\alpha} n_{R,\uparrow} \mathrm{e}^{i\sqrt{4\pi}\phi_{R,\uparrow/\downarrow}(x)},$$

where $n_{L/R}$ is the Klein factor to preserve the anticommutivity of the fermionic field. Here we introduce two bosonic fields, $\theta(x)$ and $\phi(x)$, which are dual to each other. The relations of these two fields are, $\phi(x) = \phi_R(x) + \phi_L(x)$ and $\theta(x) = \theta_R(x) + \theta_L(x)$. After the continuum field theory one can write the bosonised form of Hamiltonian as

$$\begin{aligned} H = &\int \mathrm{d}x \frac{v}{2}\left[\frac{1}{K}((\partial_x\phi)^2 + K(\partial_x\theta)^2)\right] \\ &+ \left(\frac{B}{\pi}\right)\int \mathrm{d}x\ \cos(\sqrt{4\pi}\phi) \\ &- \left(\frac{\Delta}{\pi}\right)\int \mathrm{d}x\ \cos(\sqrt{4\pi}\theta) + \left(\frac{g_u}{2\pi^2}\right) \\ &\times \int \mathrm{d}x\ \cos(4\sqrt{\pi}\phi) - \left(\frac{\mu}{\sqrt{\pi}}\right)\int \mathrm{d}x\,\partial_x\phi. \end{aligned} \tag{3}$$

This is our model Hamiltonian where $J_x = v_\mathrm{F} + \Delta$, $J_y = v_\mathrm{F} - \Delta$ and $J_z = g_u$ are coupling constants. $\theta(x)$ and $\phi(x)$ are the dual fields and

$$v = v_\mathrm{F} + \frac{g_4}{2\pi},$$

where v is the collective velocity and v_F is the Fermi velocity with

$$K = 1 - \frac{g_2}{2\pi v_\mathrm{F}}.$$

K is the Luttinger liquid parameter of the system.

Before we begin to discuss the appearance of quantum BKT transition in our system, we discuss briefly why it is necessary to study the quantum BKT transition. Here we study two different situations for our model Hamiltonian: (i) the proximity-induced superconducting gap term is absent ($\Delta = 0$) and (ii) the applied magnetic field is absent ($B = 0$). For both these cases, only sine-Gordon coupling term is present. Therefore, there is no competition between the two mutually non-local perturbations. Therefore, one can think that there is no need to study the RG to extract quantum phases and phase boundaries. But RG method is adopted for the following reason. Each of these Hamiltonians consists of two parts. The first part is the non-interacting term where the ϕ and θ fields show quadratic fluctuations and the other part of these Hamiltonians is the sine-Gordon coupling terms of either the θ or ϕ fields. The sine-Gordon coupling term lock the field either θ or ϕ in the minima of the potential well. Therefore, the system has a competition between the quadratic part of the Hamiltonian and the sine-Gordon coupling term and this competition will govern the low-energy physics of these Hamiltonians in different limits of the system.

3. Quantum Berezinskii–Kosterlitz–Thouless equations and renormalisation group equations

We consider the model Hamiltonian H (eq. (3)) with $g_u = 0$ as it has no effect on the topological state and also on the Ising state of the system [16],

$$\begin{aligned} H = &\int \mathrm{d}x \frac{v}{2}\left[\frac{1}{K}((\partial_x\phi)^2 + K(\partial_x\theta)^2)\right] \\ &+ \left(\frac{B}{\pi}\right)\int \mathrm{d}x\ \cos(\sqrt{4\pi}\phi) - \left(\frac{\Delta}{\pi}\right) \\ &\times \int \mathrm{d}x\ \cos(\sqrt{4\pi\theta}) - \left(\frac{\mu}{\sqrt{\pi}}\right)\int \mathrm{d}x\,\partial_x\phi. \end{aligned} \tag{4}$$

We consider different conditions for the coupling parameters to obtain quantum BKT and RG equations.

Case 1: For $B = 0$ with finite Δ and chemical potential μ, the Hamiltonian can be written as

$$\begin{aligned} H_1 = &\int \mathrm{d}x \frac{v}{2}\left[\frac{1}{K}(\partial_x\phi)^2 + K(\partial_x\theta)^2\right] \\ &- \left(\frac{\Delta}{\pi}\right)\int \mathrm{d}x \cos(\sqrt{4\pi}\theta(x)) - \frac{\mu}{\sqrt{\pi}}\partial_x\phi. \end{aligned} \tag{5}$$

The RG equation for this Hamiltonian can be derived as

$$\frac{\mathrm{d}\Delta}{\mathrm{d}l} = \left[2 - \frac{1}{K}\left(1 + \frac{\mu}{v\pi}\right)\right]\Delta, \qquad \frac{\mathrm{d}K}{\mathrm{d}l} = \Delta^2. \tag{6}$$

This is the first set of quantum BKT equation.

Case 2: For $\Delta = 0$ with finite B the Hamiltonian is

$$\begin{aligned} H_2 = &\int \mathrm{d}x \frac{v}{2}\left[\frac{1}{K}(\partial_x\phi)^2 + K(\partial_x\theta)^2\right] \\ &+ \left(\frac{B}{\pi}\right)\int \mathrm{d}x \cos(\sqrt{4\pi}\phi(x)). \end{aligned} \tag{7}$$

Following the same procedure, one can derive another set of quantum BKT equation,

$$\frac{dB}{dl} = (2-K)B, \qquad \frac{dK}{dl} = -B^2K^2. \tag{8}$$

Thus, we derive two sets of RG equations. There is no corrections in the RG equation for the Hamiltonian H_2 (eq. (7)) because the sine-Gordon coupling is also for the ϕ field. For this situation, one can absorb the chemical potential term in the sine-Gordon coupling.

Case 3: For both Δ and B finite, i.e, for the Hamiltonian in eq. (4), the RG equations can be obtained as

$$\begin{aligned}\frac{d\Delta}{dl} &= \left(2 - \frac{1}{K}\left(1+\frac{\mu}{v\pi^2}\right)\right)\Delta,\\ \frac{dB}{dl} &= (2-K)B,\\ \frac{dK}{dl} &= \frac{1}{2\pi^2}(\Delta^2 - K^2B^2).\end{aligned} \tag{9}$$

We refer to the Appendix for a detailed derivation of the quantum BKT equations (eqs (6) and (8)) and the whole set of RG equation (eq. (9)). It is well known that the critical theory is invariant under the rescaling. Then the singular part of the free energy density satisfies the following scaling relations:

$$f_s[\Delta, B] = e^{-2l} f_s[e^{(2-(1+\frac{\mu}{v\pi^2})/Ki)l}\Delta, e^{(2-K)l}B].$$

The scale l can be fixed from the following analytical relation, $e^{(2-1/K)l^*}\Delta = 1$. Finally, after a few steps of calculation, we arrive at the following relation:

$$\begin{aligned}f_s[\Delta, B] = {}& \Delta^{2/(2-(1+\frac{\mu}{v\pi^2})/K)}\\ & \times \quad f_s[1, \Delta^{-(2-K)/(2-(1+\frac{\mu}{v\pi^2})/K)}B].\end{aligned}$$

The equation for Majorana–Ising topological quantum phase transition is

$$\Delta^{-(2-K)/(2-(1+\frac{\mu}{v\pi^2})/K)}B \sim 1. \tag{10}$$

The phase boundary between these two quantum phases can be obtained by using the above relation, which we present in the next section.

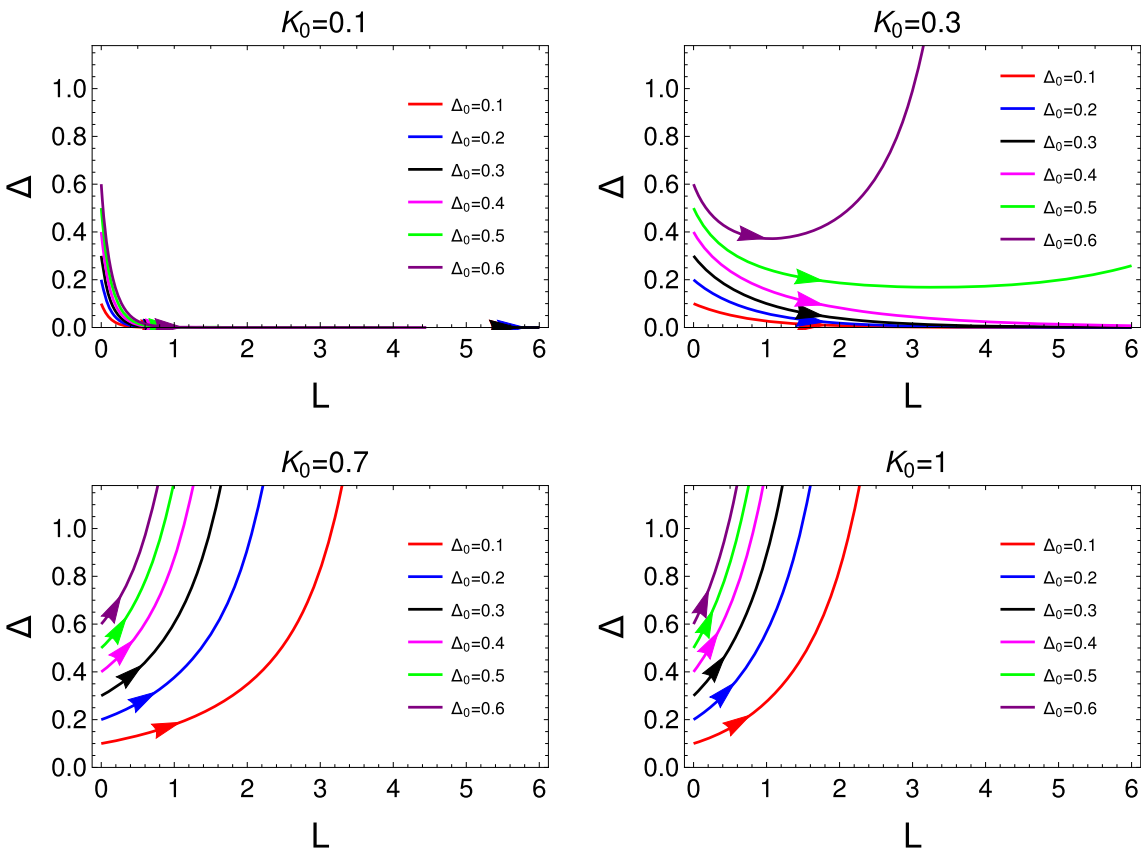

Figure 1. Variation of Δ with the length scale for $\mu = 0$ (eq. (6)). This illustrates the emergence of different quantum phases. We consider different initial values $K_0 = 0.1$ and 0.3 in the upper panel and $K_0 = 0.7$ and 1 in the lower panel for different values of Δ_0 as shown in the legend of the plot.

4. Length scale-dependent study of quantum BKT transition: Emergence of quantum phases

Emergence of quantum phases for the quantum BKT in eq. (6) with $\mu = 0$ is shown in figure 1. It shows the variation of coupling parameter Δ with the length scale which gives the evidence of emergence of topological superconducting (TS) phase of quantum matter. We present results for different initial values of K. The upper panel of figure 1 is plotted for smaller values of K_0 (0.1, 0.3), while the lower panel is for higher K_0 (0.7, 1). For $K_0 = 0.1$, the coupling parameter Δ decreases to zero with the length scale for different initial values Δ_0, driving the system to the trivial helical Luttinger liquid (HLL) phase. Our study shows that for higher values of K_0 (0.7, 1), the coupling parameter Δ increases with length scale and it is sharper as K_0 increases, indicating the emergence of TS phase in the system. Interesting behaviour can be observed for $K_0 = 0.3$ where the system tends to HLL phase for lower initial values of the coupling ($\Delta_0 = 0.1, 0.2, 0.3, 0.4$) and TS phase for higher initial values of the coupling ($\Delta_0 = 0.5, 0.6$). The coupling initially decreases driving the system to HLL phase but finally increases to TS phase as a function of length scale. This emergent phenomenon of quantum phases at different length scales can also be observed in the presence of finite chemical potential μ.

The effect of finite μ on the emergent quantum phases is shown in figure 2. The quantum BKT in eq. (6) for finite μ has the same qualitative behaviour for smaller μ as shown in the upper panel. There is a transition from HLL phase to TS phase with the length scale for $\Delta_0 = 0.6$, $\mu = 0.3$ and $K_0 = 0.3$. Similarly, the system tends to TS phase completely for higher values of K_0. In the lower panel ($K_0 = 0.3$ and $\mu = 1$), one can observe that the emergence of TS phase for large length scale is suppressed by the large value of chemical potential $\mu = 1$. The qualitative behaviour of the transition of the system to TS phase for $K_0 = 1$ remains intact even at $\mu = 1$. These results are the same as in the case of figure 2 except that the sharpness in the increasing curve of coupling, decreases for higher values of μ.

Along with the TS phase one can also observe the emergence of Ising phase with the HLL phase by considering the quantum BKT in eq. (8). Figure 3 shows the variation of coupling B, with the length

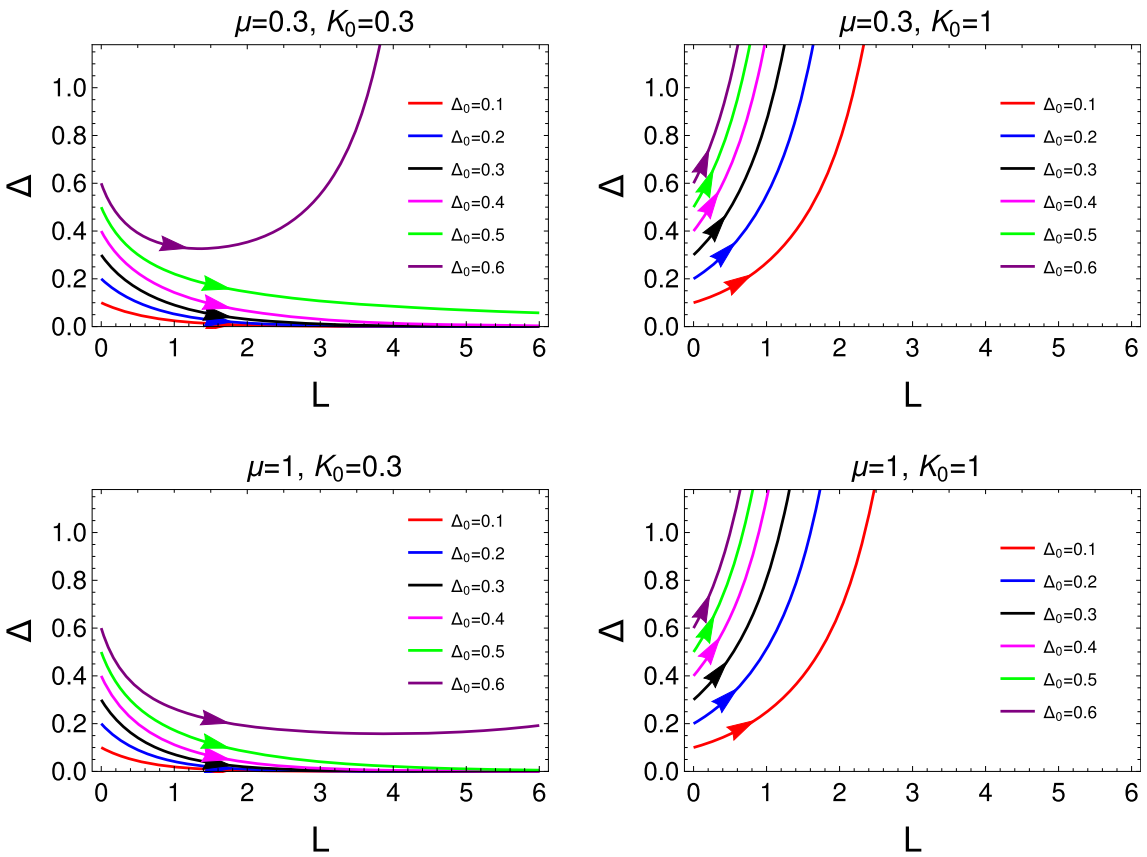

Figure 2. Variation of Δ with the length scale for $\mu \neq 0$ (eq. (6)). This illustrates the emergence of different quantum phases. We consider $\mu = 0.3$ in the upper panel and $\mu = 1$ in the lower panel for different values of K_0 and Δ_0 as shown in the legend of the plot.

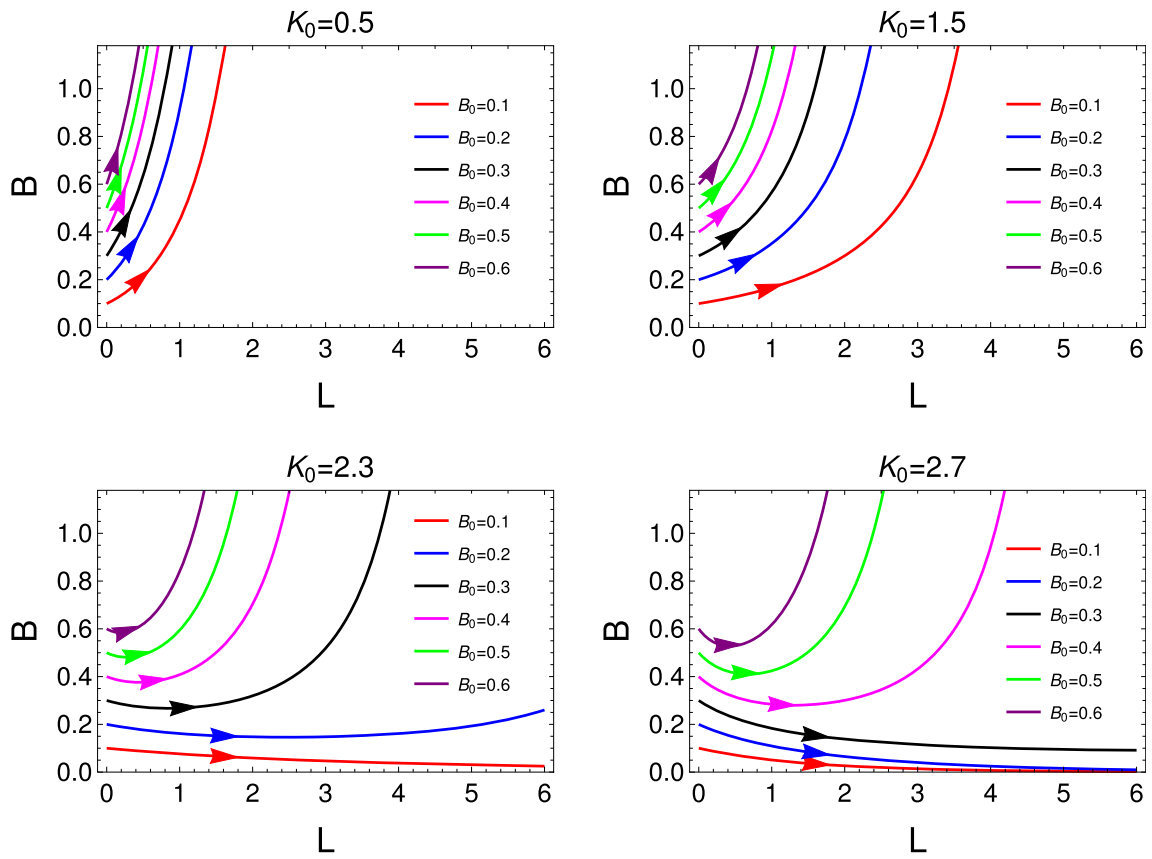

Figure 3. Variation of B with the length scale (eq. (8)). We consider different initial values $K_0 = 0.5$ and 1.5 in the upper panel and $K_0 = 2.3$ and 2.7 in the lower panel for different values of B_0 as shown in the legend of the plot.

scale which gives evidence of emergence of Ising phase of quantum matter. Unlike the previous case, the coupling B here increases for smaller values of K_0 $(0.5, 1.5)$, and the increase in B is sharper as K_0 acquire smaller values. This is clearly the evidence of Ising phase. For higher values of K_0 $(2.3, 2.7)$ the Ising phase is observed only for higher initial values of the coupling B_0. The lower initial values of the coupling tend to decrease to zero with the length scale driving the system to the trivial HLL phase.

The emergence of quantum phases for the whole set of RG equations in eq. (9) for all the coupling parameters is studied in figure 4. We set $\mu = 0$ initially and study the emergence of quantum phases. Interestingly, we find both TS and Ising phases in the system. This figure consists of two panels, the upper one is for $K_0 = 0.3$ and the lower one is for $K_0 = 1$. We find the evidence of Ising phase for smaller values of K_0 for all initial values of B_0 as shown in the upper panel. The coupling B increases with the length scale driving the system to the Ising phase.

Evidence of TS phase can also be found for higher values of K_0 as shown in the first figure of the lower panel where B increases with the length scale for $K_0 = 1$ for all initial values Δ_0. Intriguingly, the system can be found to transit between different quantum phases as a function of length scale as shown in the second figure in lower panel. Increasing the initial value to Δ_0 $(= 0.3)$ for the same K_0 and B_0 values, we find Ising phase for smaller length scale and TS phase for higher length scale. The coupling B_0 initially increases driving the system into Ising phase and finally it decreases into TS phase. However, the same is not true for $\Delta_0 = 0.3, 0.4$, which remain in Ising phase for all length scales. We observe the emergence of both Ising and TS phases for smaller and higher length scales respectively, provided the initial values of couplings satisfy the condition $B_0 \leq \Delta_0$. For $B_0 > \Delta_0$ the system collapses into a single phase depending on the value K_0. To the best of our knowledge, this is the first study in the literature where we show explicitly the emergence of two different quantum phases in different length scales.

One can also observe similar results by fixing the coupling B and varying Δ as shown in figure 5. The upper panel shows the emergence of Ising phase, where the coupling Δ decreases with the length scale for

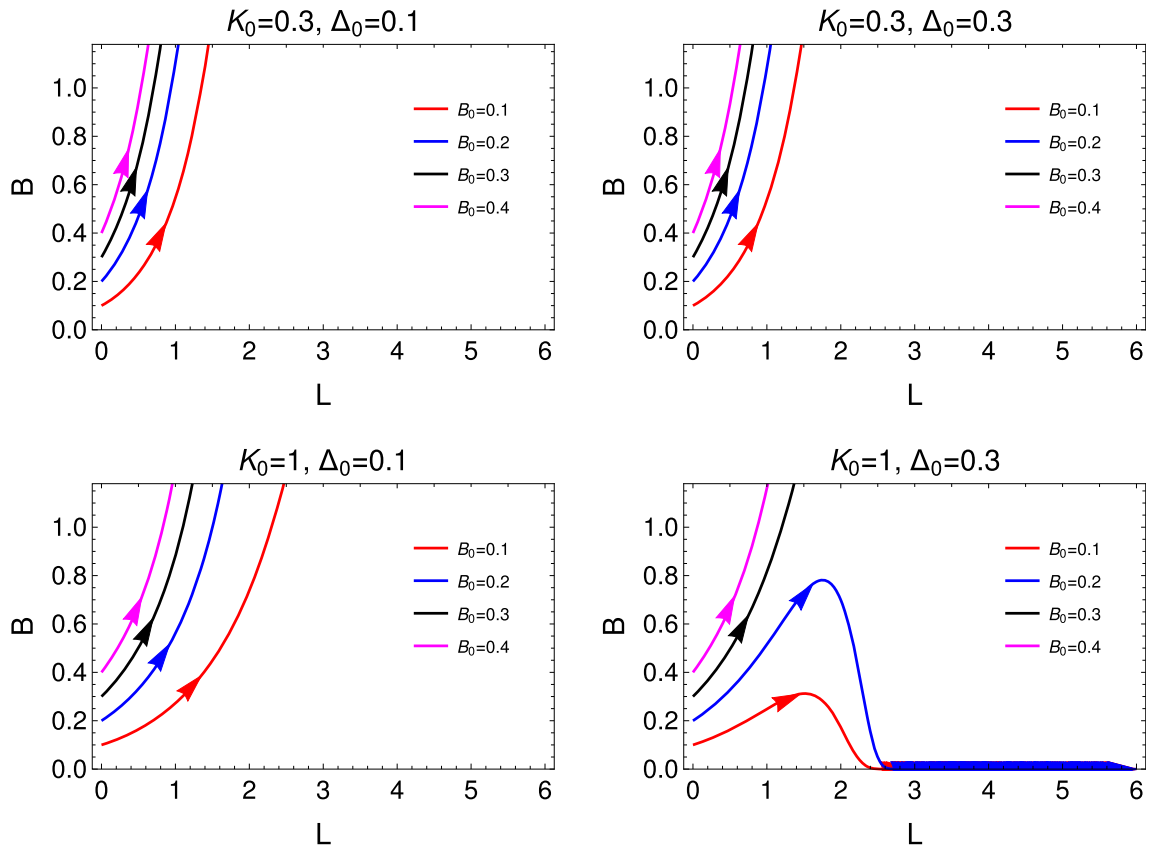

Figure 4. Variation of B with the length scale to illustrate the emergence of different quantum phases from the study of the whole set of RG equation (eq. (9)). We consider two different initial values of $K_0 = 0.3, 1$ for the upper and lower panels respectively for $\Delta_0 = 0.1, 0.3$.

both lower and higher values of B_0 at $K_0 = 0.3$. The system can be found completely driven into TS phase for lower values of B_0 at $K_0 = 1$ as shown in the first figure of the lower panel. However, the emergence of both TS and Ising phases can be observed for higher values of B_0 as shown in the second figure of the lower panel. The coupling with lower initial values ($\Delta_0 = 0.1, 0.2$) increases initially indicating the TS phase and finally drops into Ising phase. The higher initial values of coupling ($\Delta_0 = 0.3, 0.4$) drive the system completely into the TS phase for all length scales. The emergence of both TS and Ising phases with the length scale can be observed when the coupling satisfies the condition $\Delta_0 < B_0$. For $\Delta_0 \geq B_0$ the system drives into only one phase for all length scales and the transition between two quantum phases is suppressed.

Similar qualitative behaviour can be observed with finite μ. Length scale behaviour of the couplings for finite μ in eq. (9) is shown in figure 6. This figure consists of two panels, upper and lower panels are respectively for $\mu = 0.3$ and 1. In the upper panel, we observe the emergence of Ising phase as the coupling decreases with length scale for smaller value of μ ($= 0.3$). For higher value of μ ($= 1$), in the lower panel, we find the evidence of emergence of both TS and Ising phases for different length scales. As an effect of μ, the emergence of TS phase and Ising phase for lower and higher length scales respectively is observed when the coupling satisfies $\Delta_0 \leq B_0$. For $\Delta_0 > B_0$ systems drive completely into the TS phase.

In figure 7, we have presented the Majorana–Ising phase diagram for different values of chemical potential μ and Luttinger liquid parameter K. It clearly depicts the presence of TS and Ising quantum phases, whose phase boundary is varied corresponding to the value of K. The phase diagrams here show the dominance of one quantum phase over the other depending on the value of K for each value of μ. The non-interacting case ($K = 1$) separates the two phases almost equally for all values of μ. Meanwhile, the dominance of a phase over another can be seen for $K \neq 0$. For $K < 1$, the Ising phase is dominant over the TS phase which can be seen from the fact that the phase boundary curves upward which expands the Ising phase over the TS phase. Similar effect can be seen for $K > 1$ where the TS phase dominates over the Ising phase. As a consequence, the phase separation has a downward curve expanding the TS phase

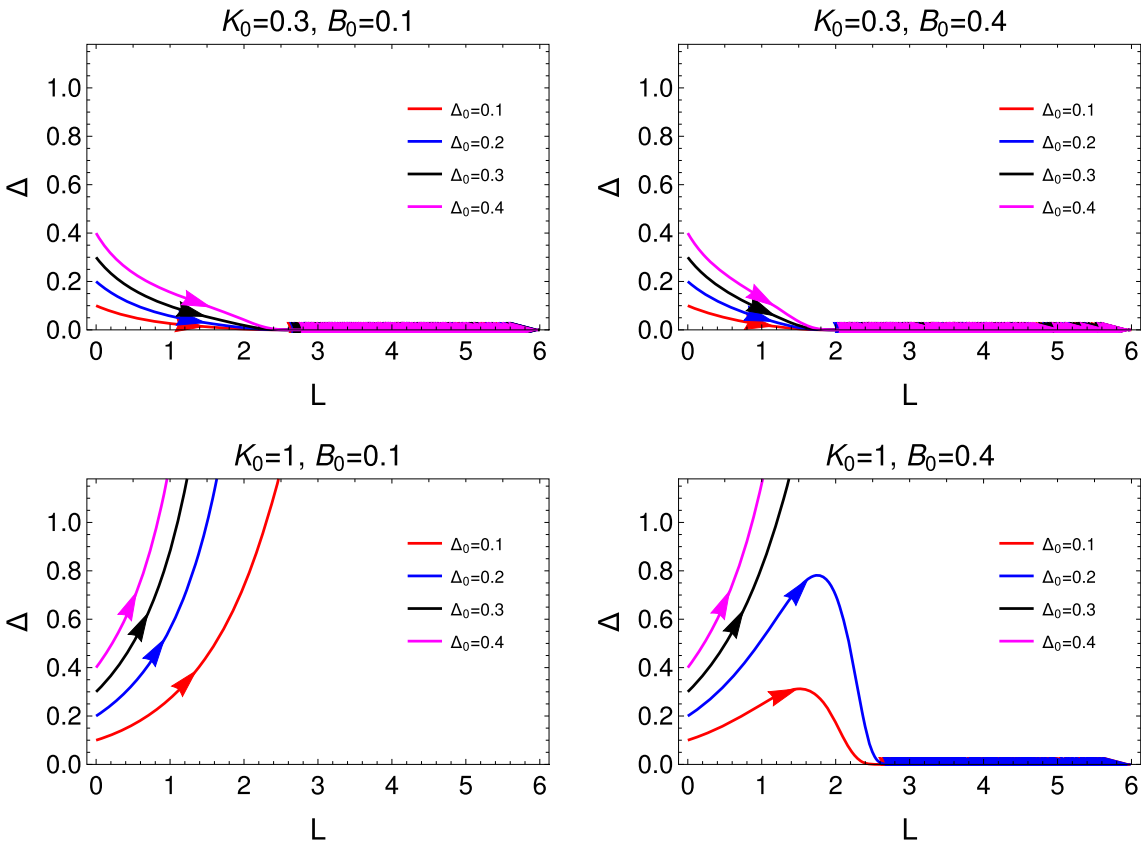

Figure 5. Variation of Δ with the length scale to illustrate the emergence of different quantum phases from the study of the whole set of RG equation (eq. (9)). We consider two different initial values of $K_0 = 0.3, 1$ for the upper and lower panels respectively for $B_0 = 0.1, 0.4$.

over the Ising phase. The transition between these quantum phases is the Majorana–Ising phase transition which can be realised from the scaling relation (eq. (10)).

We notice that, for higher values of μ the system favours the Ising phase over the TS phase. This can be verified from the case with $\mu = 2$, where the phase separation for the non-interacting limit $K = 1$ slowly curves upwards. This behaviour is prominent for higher and higher values of μ. The dependence of K and μ of this Majorana–Ising phase diagram is also consistent with the length scale-dependent quantum phases studied for the whole set of RG equations (figures 4–6). This study of Majorana–Ising transition is more enriching than the study in ref. [21] because we have presented the results of finite μ and also it is consistent with the length scale-dependent study.

5. Comparison of results between quantum BKT and whole set of RG equations

In this section, we compare the results that we have obtained in the previous section for quantum BKT and RG equations. Quantum BKT equation in eq. (6) gives rise to trivial HLL phase and TS phase in the presence and absence of chemical potential μ. Comparing these results (figures 1 and 2), we observe that the increasing value of μ will suppress the emergence of TS phase and favour the HLL phase for all initial values of coupling Δ_0. Overall, the qualitative behaviour of the coupling in driving the system into HLL phase (for lower K_0) and TS phase (for higher K_0) remains intact.

The quantum BKT equation in eq. (8) gives rise to the emergence of Ising phase. Comparing the results of two quantum BKT equations (figures 1 and 3) we observe the emergence of Ising phase for lower values of K_0, in contrast to the emergence of TS phase for higher values of K_0. Ising phase is more favourable as K_0 decreases and TS phase is more favourable as K_0 increases. Since the coupling B does not depend on μ, the emergence of Ising phase does not get suppressed by the finite chemical potential.

Intriguing results are obtained when we consider all couplings as finite, i.e., the whole set of RG equations in eq. (9). It gives rise to both TS and Ising phases for different length scales. Note that, unlike quantum BKT equations, there is no evidence of HLL phase in RG equations. Keeping the coupling B constant we get Majorana–Ising transition [15] when the couplings

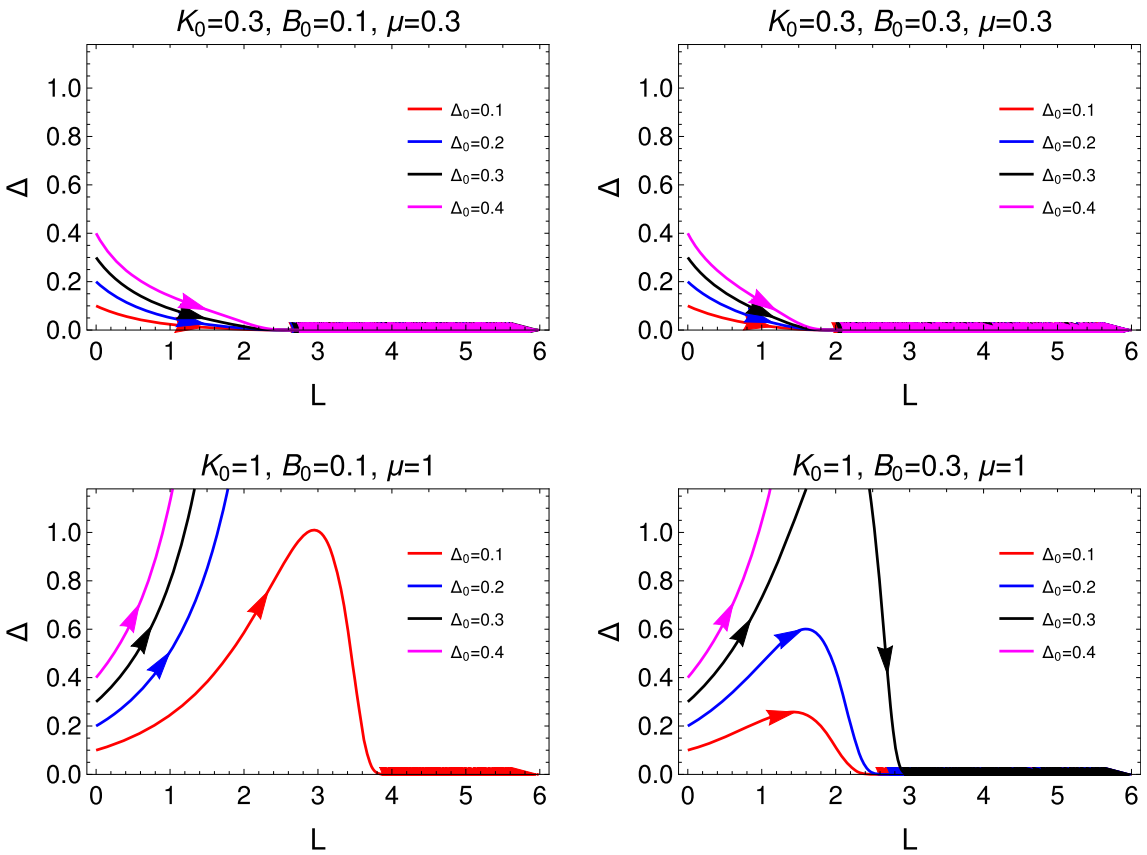

Figure 6. Variation of Δ with the length scale for $\mu \neq 0$, to illustrate the emergence of different quantum phases from the study of the whole set of RG equation (eq. (9)). We consider two different initial values of $K_0 = 0.3, 1$ and $\mu = 0.3, 1$ for the upper and lower panels respectively for $B_0 = 0.1, 0.3$.

satisfy the condition $\Delta_0 < B_0$ (figure 5). This condition for Majorana–Ising transition is modified into $\Delta_0 \leq B_0$ in the presence of finite μ (figure 6). Fixing Δ constant and varying B results in the Ising–Majorana transition. This transition occurs for $B_0 < \Delta_0$ (figure 4). Since μ has no effect on B the condition for Ising–Majorana transition does not get modified. Emergence of quantum phases (TS and Ising phases) for different length scales in the RG equations occurs for different coupling conditions. This is favourable only for higher values of K_0.

6. Experimental possibilities

Here we discuss the experimental possibilities relevant to the present length scale study of the helical edge mode physics. The physics of edge states of a topological insulator can be experimentally observed as a manifestation of quantised resistance appearing due to the quantum spin-Hall effect. The electron transport along the sample edge can be observed when the Fermi energy lies within the bulk energy gap at sufficiently low temperature. The quantised Hall resistance has been measured to be $h/2e^2$ (where e is the electron charge and h is the Planck's constant) in the multiterminal transport experiments [12]. The quantum plateau observed is the same for different sample sizes, confirming that the transport indeed occurs via edge states. The spin polarisation of edge states can be observed using a split-gate technique to combine two T-shaped bars, one in the quantum spin-Hall regime and the other one in the non-topological spin-Hall regime. Using two of the terminals for current injection and the other two as voltage probes, one can observe the accumulation of spin-up and spin-down electrons on opposite sides of the sample.The quantised multiterminal resistance again confirms the spin-polarisation of the helical edge states.

The helical edge states of the topological insulator can be mapped in real space by imaging techniques such as scanning superconducting quantum interference device (SQUID) [28,29]. The edge and bulk electron transport can be distinguished in this experimental technique. One can visualise the bulk-dominated and edge-dominated transport using gate voltage. The bulk transport can be observed when the gate voltage brings the Fermi level

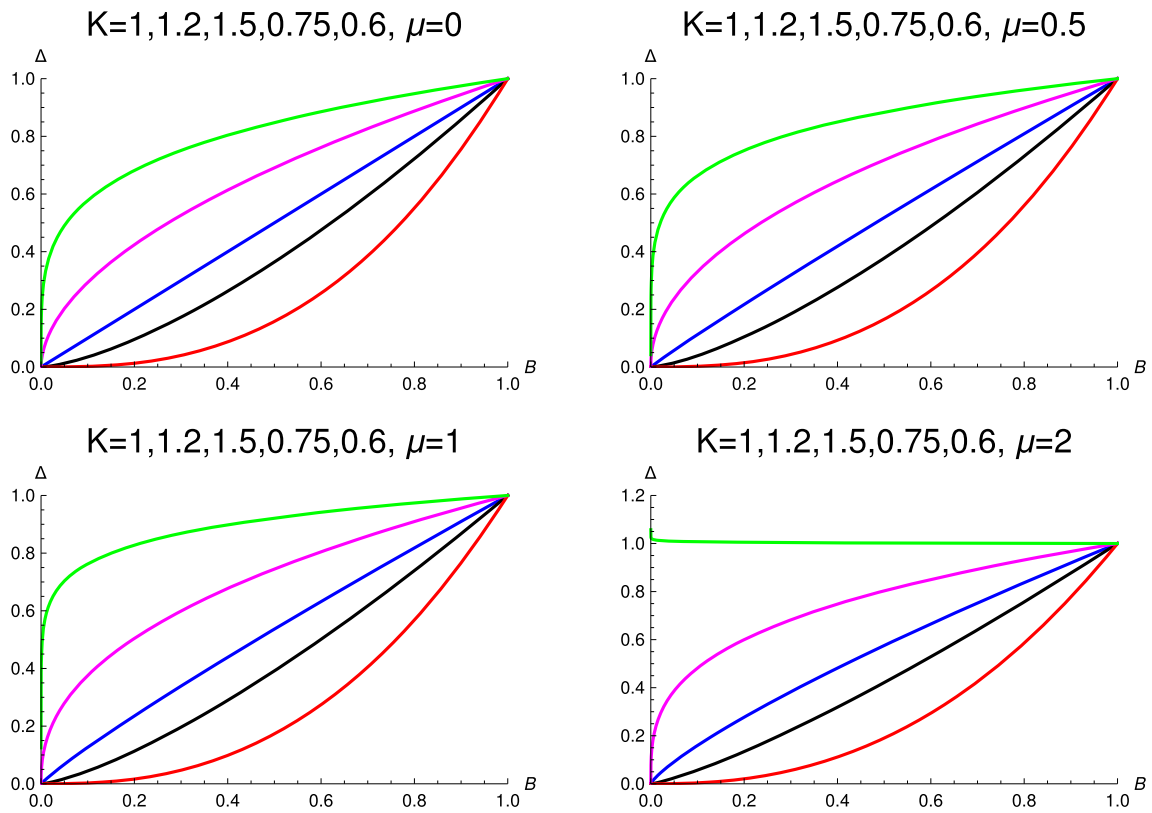

Figure 7. Phase diagram for $\mu = 0, 0.5, 1, 2$. Each figure consists of five different curves for different values of K represented in blue ($K = 1$), black ($K = 1.2$), red ($K = 1.5$), magenta ($K = 0.75$), green ($K = 0.6$).

into either valance band or conduction band, whereas the edge transport can be observed when the gate voltage brings the Fermi level into the bulk gap.

More extensive observation and the distinction between gapless helical edge states and insulating bulk states is possible in the experiments involving hybrid superconducting topological insulator devices. This experimental set-up allows one to find Majorana zero modes which can be beneficial for quantum computation [30]. Strong signatures of helical liquid states can be found by observing perfect Andreev reflection in superconductor quantum spin-Hall insulator–superconductor junctions using InAs/GaSb. In 3D materials, it is an even more challenging task to differentiate the bulk and edge contributions to the transport. Therefore, angle-resolved photoemission spectroscopy (ARPES), where a probe that couples mainly to the surface is used to detect the quantised edge conductance [31]. The spin polarisation of the surface states can be detected by analysing the energy, momentum and spin of electrons ejected from high-energy photons.

The emergence of different quantum phases discussed in this study can be realised by probing these devices to different length scales. Observing the transport properties of the edge states and bulk states of the samples for different length scales, one can identify the HLL, TS and Ising phases studied in this work. The dominant edge transport can be observed only when the system is in the TS phase and the dominant bulk transport can be observed when the system is in either the HLL or the Ising phase.

7. Conclusion

We have presented a detailed study of emergence of quantum phases at different length scales by solving quantum BKT and whole set of RG equations. We have observed the emergence of topological superconducting phase, Ising phase and also the helical Luttinger liquid phase from these quantum BKT equations. Here there is no evidence of Majorana–Ising transition. However, Majorana–Ising transition is found in the study of emergence of quantum phases for the whole set of RG equations. We have also presented the Majorana–Ising phase boundary from the analysis of the scaling relations between two fields. We have shown explicitly the importance of Luttinger liquid parameter and the condition between the couplings which result in the emergence of different quantum phases for different length scales. This work provides a new perspective on the study of the topological state of quantum matter.

Acknowledgements

RRK, SR and SS would like to acknowledge Mr N Prakash and Prof. R Srikanth for reading the manuscript critically. RRK, SR and SS also acknowledge RRI library for the books and journals and ICTS for Lectures/seminars/workshops/conferences/discussion meetings of different aspects of physics. SS would like to acknowledge DST (EMR/2017/000898) for the support. RRK and SR would like to thank Admar Mutt Education Foundation for the scholarship.

Appendix A. Derivation of RG equations for the model Hamiltonian

We consider the bosonised model Hamiltonian with $g_u = 0$ after rescaling the fields,

$$\phi' = \frac{\phi}{\sqrt{K}}$$

and

$$\theta' = \sqrt{K}\theta.$$

Now the model Hamiltonian can be rewritten as

$$H = \frac{v}{2}[(\partial_x\phi')^2 + (\partial_x\theta')^2] - \mu\sqrt{\frac{K}{\pi}}\partial_x\phi' + \frac{B}{\pi}\cos(\sqrt{4\pi K}\phi') - \frac{\Delta}{\pi}\cos\left(\sqrt{\frac{4\pi}{K}}\theta'\right), \quad \text{(A.1)}$$

where $\theta(x)$ and $\phi(x)$ are the dual fields and K is the Luttinger liquid parameter of the system. Writing the Lagrangian using the Hamilton's equations,

$$\partial_x\theta' = -\frac{1}{v}\partial_t\phi'$$

and

$$\partial_x\phi' = -\frac{1}{v}\partial_t\theta'$$

leads to

$$\mathcal{L}_0^{(\phi)} = \Pi_{\phi'}\partial_t\phi' - H_0' = \tfrac{1}{2}[v^{-1}(\partial_t\phi')^2 - v(\partial_x\phi')^2],$$
$$\mathcal{L}_0^{(\theta)} = \Pi_{\theta'}\partial_t\theta' - H_0' = \tfrac{1}{2}[v^{-1}(\partial_t\theta')^2 - v(\partial_x\theta')^2]. \quad \text{(A.2)}$$

Thus, the complete form of $\mathcal{L}_0 = \mathcal{L}_0^{(\phi)} + \mathcal{L}_0^{(\theta)}$ in terms of imaginary time, i.e, $\tau = it$, can be written as

$$\mathcal{L}_0 = -\frac{1}{4}[v^{-1}(\partial_\tau\phi')^2 + v^{-1}(\partial_\tau\theta')^2 + v(\partial_x\phi')^2 + v(\partial_x\theta')^2].$$

Lagrangian of the interaction terms $\mathcal{L}_{\text{int}} = -H_{\text{int}}$ are

$$\mathcal{L}_{\text{int}} = -\frac{i\mu}{v}\sqrt{\frac{K}{\pi}}\partial_\tau\theta' - \frac{B}{\pi}\cos(\sqrt{4\pi K}\phi') + \frac{\Delta}{\pi}\cos\left(\sqrt{\frac{4\pi}{K}}\theta'\right). \quad \text{(A.3)}$$

Now we write the partition function $\mathcal{Z}$ as

$$\mathcal{Z} = \int \mathcal{D}\phi\mathcal{D}\theta \mathrm{e}^{-S_E[\phi,\theta]}, \quad \text{(A.4)}$$

where

$$S_E = \int \mathrm{d}\tau\, \mathrm{d}x\mathcal{L} = \int \mathrm{d}\tau\, \mathrm{d}x(\mathcal{L}_0 + \mathcal{L}_{\text{int}})$$

is the Euclidean action. Thus, we have

$$\mathcal{Z} = \int \mathcal{D}\phi\mathcal{D}\theta\ \exp\left[-\int_{-\Lambda}^{\Lambda}\frac{\mathrm{d}\omega}{2\pi}|\omega|\left(\frac{|\phi(\omega)|^2}{2K} + \frac{K|\theta(\omega)|^2}{2}\right) + \int \mathrm{d}\tau\ (\mathcal{L}_{\text{int}})\right]. \quad \text{(A.5)}$$

Now we divide the fields into slow and fast modes and integrate out the fast modes. The field $\phi(\tau) = \phi_s(\tau) + \phi_f(\tau)$ and $\theta(\tau) = \theta_s(\tau) + \theta_f(\tau)$, where

$$\phi_s(\tau) = \int_{-\Lambda/b}^{\Lambda/b}\frac{\mathrm{d}\omega}{2\pi}\mathrm{e}^{-i\omega\tau}\phi(\omega),$$
$$\phi_f(\tau) = \int_{\Lambda/b<|\omega_n|<\Lambda}\frac{\mathrm{d}\omega}{2\pi}\mathrm{e}^{-i\omega\tau}\phi(\omega)$$
$$\theta_s(\tau) = \int_{-\Lambda/b}^{\Lambda/b}\frac{\mathrm{d}\omega}{2\pi}\mathrm{e}^{-i\omega\tau}\theta(\omega),$$
$$\theta_f(\tau) = \int_{\Lambda/b<|\omega_n|<\Lambda}\frac{\mathrm{d}\omega}{2\pi}\mathrm{e}^{-i\omega\tau}\theta(\omega).$$

Thus, $\mathcal{Z}$ can be written as

$$\mathcal{Z} = \int \mathcal{D}\phi_s\mathcal{D}\phi_f\mathcal{D}\theta_s\mathcal{D}\theta_f \times \mathrm{e}^{-S_s(\phi_s,\theta_s)}\mathrm{e}^{-S_f(\phi_f,\theta_f)}\mathrm{e}^{-S_{int}(\phi,\theta)}. \quad \text{(A.6)}$$

Now the effective action can be written as

$$S_{\text{eff}}(\phi_s,\theta_s) = S_s(\phi_s,\theta_s) - \ln\langle\mathrm{e}^{-S_{\text{int}}(\phi,\theta)}\rangle_f. \quad \text{(A.7)}$$

Writing the cumulant expansion up to the second order, we have

$$S_{\text{eff}}(\phi_s,\theta_s) = S_s(\phi_s,\theta_s) + \langle S_{\text{int}}(\phi,\theta)\rangle_f - \frac{1}{2}(\langle S_{\text{int}}^2(\phi,\theta)\rangle_f - \langle S_{\text{int}}(\phi,\theta)\rangle_f^2). \quad \text{(A.8)}$$

At first, we calculate the first-order cumulant expansion

$$\langle S_{\rm int}(\phi,\theta)\rangle_f = \int \mathrm{d}\tau \left\langle \frac{i\mu}{v\sqrt{\pi}}\partial_\tau\theta\right\rangle_f + \int \mathrm{d}\tau \frac{B}{\pi}\langle\cos(\sqrt{4\pi}\phi(\tau))\rangle_f - \int \mathrm{d}\tau \frac{\Delta}{\pi}\langle\cos(\sqrt{4\pi}\theta(\tau))\rangle_f. \quad \text{(A.9)}$$

The second term can be written as

$$\begin{aligned}\langle S_B(\phi_s,\phi_f)\rangle &= \int \mathrm{d}\tau \left(\frac{B}{\pi}\right)\int \mathcal{D}\phi_f\, {}^{-S_f[\phi_f]}\cos(\sqrt{4\pi}\phi(\tau))\\ &= \frac{B}{2\pi}\int \mathrm{d}\tau \left\{\mathrm{e}^{i\sqrt{4\pi}\phi_s(\tau)}\mathrm{e}^{-\int_f \frac{\mathrm{d}\omega}{2\pi}\frac{4\pi}{2}\frac{K}{|\omega|}} + \text{H.c.}\right\}\\ &= b^{-K}\int \mathrm{d}\tau \left(\frac{B}{\pi}\right)\cos[\sqrt{4\pi}\phi_s(\tau)].\end{aligned}$$

Similarly, for coupling Δ we have

$$\langle S_\Delta(\theta_s,\theta_f)\rangle = b^{-1/K}\int \mathrm{d}\tau \left(\frac{\Delta}{\pi}\right)\cos[\sqrt{4\pi}\theta_s(\tau)]. \quad \text{(A.10)}$$

Thus, the first-order cumulant expansions can be rewritten as

$$\langle S_{\rm int}(\phi,\theta)\rangle_f = b^{-K}\int \mathrm{d}\tau \left(\frac{B}{\pi}\cos(\sqrt{4\pi}\phi_s(\tau))\right) - b^{-1/K}\int \mathrm{d}\tau \left(\frac{\Delta}{\pi}\cos(\sqrt{4\pi}\theta_s(\tau))\right). \quad \text{(A.11)}$$

Now we calculate the second-order cumulant expansion which has the following terms:

$$\begin{aligned}&-\frac{1}{2}(\langle S_{\rm int}^2\rangle - \langle S_{\rm int}\rangle^2) = -\frac{1}{2}\int \mathrm{d}\tau\,\mathrm{d}\tau'\\ &\times\left(-\frac{\mu^2}{v^2\pi}\left\langle\partial_\tau\phi(\tau)\partial_{\tau'}\phi(\tau')\right\rangle - \langle\partial_\tau\phi(\tau)\rangle\left\langle\partial_{\tau'}\phi(\tau')\right\rangle\right)\\ &-\frac{1}{2}\int \mathrm{d}\tau\,\mathrm{d}\tau'\left(\frac{B^2}{\pi^2}\langle\cos(\sqrt{4\pi}\phi(\tau))\cos(\sqrt{4\pi}\phi(\tau'))\rangle\right.\\ &\left.-\langle\cos(\sqrt{4\pi}\phi(\tau))\rangle\langle\cos(\sqrt{4\pi}\phi(\tau'))\rangle\right)\\ &-\frac{1}{2}\int \mathrm{d}\tau\,\mathrm{d}\tau'\left(\frac{\Delta^2}{\pi^2}\langle\cos(\sqrt{4\pi}\theta(\tau))\cos(\sqrt{4\pi}\theta(\tau'))\rangle\right.\\ &\left.-\langle\cos(\sqrt{4\pi}\theta(\tau))\rangle\langle\cos(\sqrt{4\pi}\theta(\tau'))\rangle\right)\\ &-\frac{1}{2}\int \mathrm{d}\tau\,\mathrm{d}\tau'\left(\frac{i\mu B}{v\sqrt{\pi}\pi}\langle\partial_\tau\phi(\tau)\cos(\sqrt{4\pi}\phi(\tau'))\rangle\right.\\ &\left.\times\langle\partial_\tau\phi(\tau)\rangle - \langle\cos(\sqrt{4\pi}\phi(\tau'))\rangle\right)\\ &-\frac{1}{2}\int \mathrm{d}\tau\,\mathrm{d}\tau'\left(-\frac{i\mu\Delta}{v\sqrt{\pi}\pi}\langle\partial_\tau\phi(\tau)\cos(\sqrt{4\pi}\theta(\tau'))\rangle\right.\\ &\left.-\langle\partial_\tau\phi(\tau)\rangle\langle\cos(\sqrt{4\pi}\theta(\tau'))\rangle\right)\\ &-\frac{1}{2}\int \mathrm{d}\tau\,\mathrm{d}\tau'\left(\frac{Bi\mu}{\pi v\sqrt{\pi}}\langle\cos(\sqrt{4\pi}\phi(\tau))\partial_{\tau'}\phi(\tau')\rangle\right.\\ &\left.-\langle\cos(\sqrt{4\pi}\phi(\tau))\rangle\left\langle\partial_{\tau'}\phi(\tau')\right\rangle\right)\\ &-\frac{1}{2}\int \mathrm{d}\tau\mathrm{d}\tau'\left(-\frac{B\Delta}{\pi^2}\langle\cos(\sqrt{4\pi}\phi(\tau))\cos(\sqrt{4\pi}\theta(\tau'))\rangle\right.\\ &\left.-\langle\cos(\sqrt{4\pi}\phi(\tau))\rangle\langle\cos(\sqrt{4\pi}\theta(\tau'))\rangle\right)\\ &-\frac{1}{2}\int \mathrm{d}\tau\,\mathrm{d}\tau'\left(-\frac{\Delta i\mu}{\pi v\sqrt{\pi}}\langle\cos(\sqrt{4\pi}\theta(\tau))\partial_{\tau'}\phi(\tau')\rangle\right.\\ &\left.-\langle\cos(\sqrt{4\pi}\theta(\tau))\rangle\left\langle\partial_{\tau'}\phi(\tau')\right\rangle\right)\\ &-\frac{1}{2}\int \mathrm{d}\tau\mathrm{d}\tau'\left(-\frac{\Delta B}{\pi^2}\langle\cos(\sqrt{4\pi}\theta(\tau))\cos(\sqrt{4\pi}\phi(\tau'))\rangle\right.\\ &\left.-\langle\cos(\sqrt{4\pi}\theta(\tau))\rangle\langle\cos(\sqrt{4\pi}\phi(\tau'))\rangle\right). \quad \text{(A.12)}\end{aligned}$$

Now we calculate each term separately. B^2 term can be written as

$$\begin{aligned}&-\frac{1}{2}\int \mathrm{d}\tau\,\mathrm{d}\tau'\left(\frac{B^2}{\pi^2}\langle\cos(\sqrt{4\pi}\phi(\tau))\cos(\sqrt{4\pi}\phi(\tau'))\rangle\right.\\ &\left.-\langle\cos(\sqrt{4\pi}\phi(\tau))\rangle\langle\cos(\sqrt{4\pi}\phi(\tau'))\rangle\right)\\ &= -\frac{B^2}{2\pi^2}\int \mathrm{d}\tau\,\mathrm{d}\tau'[\cos\sqrt{4\pi}[\phi_s(\tau)+\phi_s(\tau')]\\ &\times(\mathrm{e}^{-2\pi\langle(\phi_f(\tau)+\phi_f(\tau'))^2\rangle} - \mathrm{e}^{-2\pi[\langle\phi_f^2(\tau)\rangle+\langle\phi_f^2(\tau')\rangle]})]\\ &-\frac{B^2}{2\pi^2}\int \mathrm{d}\tau\,\mathrm{d}\tau'[\cos\sqrt{4\pi}[\phi_s(\tau)-\phi_s(\tau')]\\ &\times(\mathrm{e}^{-2\pi\left\langle(\phi_f(\tau)-\phi_f(\tau'))^2\right\rangle} - \mathrm{e}^{-2\pi[\left\langle\phi_f^2(\tau)\right\rangle+\left\langle\phi_f^2(\tau')\right\rangle]})]. \quad \text{(A.13)}\end{aligned}$$

The correlation function can be calculated as

$$\mathrm{e}^{-2\pi\left\langle(\phi_f(\tau)+\phi_f(\tau'))^2\right\rangle} = b^{-4K},$$
$$\mathrm{e}^{-2\pi\left\langle(\phi_f(\tau)-\phi_f(\tau'))^2\right\rangle} = 1$$

and

$$\mathrm{e}^{-2\pi[\left\langle\phi_f^2(\tau)\right\rangle+\left\langle\phi_f^2(\tau')\right\rangle]} = b^{-2K}.$$

Thus, by setting $\tau' \to \tau$ we have

$$-\frac{1}{2}\int \mathrm{d}\tau\,\mathrm{d}\tau'\Bigg(\frac{B^2}{\pi^2}\langle\cos(\sqrt{4\pi}\phi(\tau))\cos(\sqrt{4\pi}\phi(\tau'))\rangle - \langle\cos(\sqrt{4\pi}\phi(\tau))\rangle\langle\cos(\sqrt{4\pi}\phi(\tau'))\rangle\Bigg)$$
$$= -\frac{B^2}{2\pi^2}\int \mathrm{d}\tau\Bigg[\cos[2\sqrt{4\pi}\phi_s(\tau)] \times (b^{-4K} - b^{-2K}) + \Bigg[1 - \frac{1}{2}(\partial_\tau\phi_s)^2\Bigg](1 - b^{-2K})\Bigg]. \tag{A.14}$$

Here we have

$$\frac{\mathrm{d}}{\mathrm{d}\tau}\cos[\sqrt{4\pi}(\phi_s(\tau) - \phi_s(\tau'))] = -\sin[\sqrt{4\pi}(\phi_s(\tau) - \phi_s(\tau'))]\left(-\frac{\partial\phi_s}{\partial\tau'}\right). \tag{A.15}$$

$$\frac{\mathrm{d}^2}{\mathrm{d}\tau'^2}\cos[\sqrt{4\pi}(\phi_s(\tau) - \phi_s(\tau'))] = -\cos[\sqrt{4\pi}(\phi_s(\tau) - \phi_s(\tau'))]\left(-\frac{\partial\phi_s}{\partial\tau'}\right)^2 + \sin[\sqrt{4\pi}(\phi_s(\tau) - \phi_s(\tau'))]\left(-\frac{\partial^2\phi_s}{\partial\tau'^2}\right)^2. \tag{A.16}$$

As $\tau \to \tau'$

$$\to \left(\frac{\partial\phi_s}{\partial\tau'}\right)^2. \tag{A.17}$$

Thus, we have $\cos\sqrt{4\pi}[\phi_s(\tau) - \phi_s(\tau')] = 1 - \frac{1}{2}(\partial_\tau\phi_s)^2$. The first part of the second term is field-independent. This term can be neglected and we remain with

$$-\frac{1}{2}\int \mathrm{d}\tau\,\mathrm{d}\tau'\Bigg(\frac{B^2}{\pi^2}\langle\cos(\sqrt{4\pi}\phi(\tau))\cos(\sqrt{4\pi}\phi(\tau'))\rangle - \langle\cos(\sqrt{4\pi}\phi(\tau))\rangle\langle\cos(\sqrt{4\pi}\phi(\tau'))\rangle\Bigg)$$
$$= \frac{B^2}{4\pi^2}(1 - b^{-2K})\int \mathrm{d}\tau(\partial_\tau\phi_s)^2 - \frac{B^2}{2\pi^2}(b^{-4K} - b^{-2K})\int \mathrm{d}\tau\cos[\sqrt{16\pi}\phi_s(\tau)]. \tag{A.18}$$

Similarly, one can also follow the same procedure for Δ^2 term.

$$-\frac{1}{2}\int \mathrm{d}\tau\,\mathrm{d}\tau'\Bigg(\frac{\Delta^2}{\pi^2}\langle\cos(\sqrt{4\pi}\theta(\tau))\cos(\sqrt{4\pi}\theta(\tau'))\rangle - \langle\cos(\sqrt{4\pi}\theta(\tau))\rangle\langle\cos(\sqrt{4\pi}\theta(\tau'))\rangle\Bigg) = \frac{\Delta^2}{4\pi^2}(1 - b^{-2/K})\int \mathrm{d}\tau(\partial_\tau\theta_s)^2. \tag{A.19}$$

Now we calculate $\Delta i\mu$ term,

$$-\frac{1}{2}\int \mathrm{d}\tau\,\mathrm{d}\tau'\Bigg(-\frac{\Delta i\mu}{\pi v\sqrt{\pi}}\langle\cos(\sqrt{4\pi}\theta(\tau))\partial_{\tau'}\theta(\tau')\rangle - \langle\cos(\sqrt{4\pi}\theta(\tau))\rangle\left\langle\partial_{\tau'}\theta(\tau')\right\rangle\Bigg)$$
$$= \frac{\Delta i\mu}{2\pi v\sqrt{\pi}}\int \mathrm{d}\tau\,\mathrm{d}\tau'[\langle\cos[\sqrt{4\pi}\theta(\tau)](\partial_{\tau'}\theta_s(\tau') + \partial_{\tau'}\theta_f(\tau'))\rangle] - \frac{\Delta i\mu}{2\pi v\sqrt{\pi}}\int \mathrm{d}\tau\,\mathrm{d}\tau'[\langle\cos[\sqrt{4\pi}\theta(\tau)]\rangle\langle\partial_{\tau'}\theta_s(\tau') + \partial_{\tau'}\theta_f(\tau')\rangle]$$
$$= \frac{\Delta i\mu}{2\pi v\sqrt{\pi}}\int \mathrm{d}\tau\,\mathrm{d}\tau'[\langle\cos[\sqrt{4\pi}\theta(\tau)]\partial_{\tau'}\theta_f(\tau')\rangle]. \tag{A.20}$$

The correlation function $\langle\cos[\sqrt{4\pi}\theta(\tau)]\partial_{\tau'}\theta_f(\tau')\rangle$ can be calculated as

$$\langle\cos[\sqrt{4\pi}\theta(\tau)]\partial_{\tau'}\theta_f(\tau')\rangle = \lim_{\epsilon\to 0}\frac{1}{2i\epsilon\sqrt{\pi}}\partial_{\tau'}\langle\mathrm{e}^{2i\epsilon\sqrt{\pi}\theta_f(\tau')}\cos[\sqrt{4\pi}\theta(\tau)]\rangle = -2\sqrt{\pi}\sin[\sqrt{4\pi}\theta_s(\tau)]\partial_{\tau'}\langle\theta_f(\tau')\theta_f(\tau)\rangle\mathrm{e}^{-2\pi\left\langle\theta_f^2(\tau)\right\rangle}. \tag{A.21}$$

Thus, we have

$$= -\frac{\Delta i\mu}{\pi v}\int \mathrm{d}\tau\,\mathrm{d}\tau'\sin[\sqrt{4\pi}\theta_s(\tau)]\partial_{\tau'}\langle\theta_f(\tau')\theta_f(\tau)\rangle \times \mathrm{e}^{-2\pi\left\langle\theta_f^2(\tau)\right\rangle}$$
$$= -\frac{\Delta i\mu}{\pi v}\int \mathrm{d}\tau\sin[\sqrt{4\pi}\theta_s(\tau)]\left(-\frac{1}{2\pi K}\ln b\right) \times \mathrm{e}^{-2\pi\left(-\frac{1}{2\pi K}\ln b\right)}$$
$$= \frac{\Delta i\mu}{2\pi^2 v}\int \mathrm{d}\tau\sin[\sqrt{4\pi}\theta_s(\tau)](\mathrm{e}^{\frac{1}{K}\ln b} - 1)(\mathrm{e}^{-\frac{1}{K}\ln b})$$
$$= -\frac{\Delta\mu}{2\pi^2 v}(1 - b^{-1/K})\int \mathrm{d}\tau\cos[\sqrt{4\pi}\theta_s(\tau)].$$

Thus, the combined $\Delta i\mu$ and $i\mu\Delta$ terms is

$$-\frac{1}{2}\int \mathrm{d}\tau\,\mathrm{d}\tau'\Big(-\frac{\Delta i\mu}{\pi v\sqrt{\pi}}\langle\cos(\sqrt{4\pi}\theta(\tau))\partial_{\tau'}\theta(\tau')\rangle - \langle\cos(\sqrt{4\pi}\theta(\tau))\rangle\left\langle\partial_{\tau'}\theta(\tau')\right\rangle\Big) = -\frac{\Delta\mu}{\pi^2 v}(1-b^{-1/K})\int \mathrm{d}\tau\cos[\sqrt{4\pi}\theta_s(\tau)]. \quad \text{(A.22)}$$

In the case of $Bi\mu$, the correlation function $\langle\phi_f(\tau)\theta_f(\tau')\rangle$ is

$$\begin{aligned}&\langle\phi_f(\tau)\theta_f(\tau')\rangle\\ &= \langle(\phi_{R\uparrow}+\phi_{L\downarrow})(\phi'_{R\uparrow}-\phi'_{L\downarrow})\rangle\\ &=\langle\phi_{R\uparrow}\phi'_{R\uparrow}-\phi_{R\uparrow}\phi'_{L\downarrow}+\phi_{L\downarrow}\phi'_{R\uparrow}-\phi_{L\downarrow}\phi'_{L\downarrow}\rangle=0.\end{aligned} \quad \text{(A.23)}$$

Thus, the combined $Bi\mu$ and $i\mu B$ terms are equal to zero. Now, we calculate the term $B\Delta$,

$$\begin{aligned}&-\frac{1}{2}\int \mathrm{d}\tau\mathrm{d}\tau'\Big(-\frac{B\Delta}{\pi^2}\langle\cos(\sqrt{4\pi}\phi(\tau))\cos(\sqrt{4\pi}\theta(\tau'))\rangle - \langle\cos(\sqrt{4\pi}\phi(\tau))\rangle\langle\cos(\sqrt{4\pi}\theta(\tau'))\rangle\Big)\\ &= \frac{B\Delta}{4\pi^2}\int \mathrm{d}\tau\,\mathrm{d}\tau'[\cos\sqrt{4\pi}[\phi_s(\tau)+\theta_s(\tau')]\\ &\quad\times(\mathrm{e}^{-2\pi\langle(\phi_f(\tau)+\theta_f(\tau'))^2\rangle}-\mathrm{e}^{-2\pi[\langle\phi_f^2(\tau)\rangle+\langle\theta_f^2(\tau')\rangle]})]\\ &\quad+\frac{B\Delta}{4\pi^2}\int \mathrm{d}\tau\,\mathrm{d}\tau'[\cos\sqrt{4\pi}[\phi_s(\tau)-\theta_s(\tau')]\\ &\quad\times(\mathrm{e}^{-2\pi\langle(\phi_f(\tau)-\theta_f(\tau'))^2\rangle}-\mathrm{e}^{-2\pi[\langle\phi_f^2(\tau)\rangle+\langle\theta_f^2(\tau')\rangle]})].\end{aligned} \quad \text{(A.24)}$$

Here the correlation function,

$$\mathrm{e}^{-2\pi\langle(\phi_f(\tau)\pm\theta_f(\tau'))^2\rangle} = \mathrm{e}^{-2\pi\langle\phi_f^2(\tau)\rangle+\langle\theta_f^2(\tau')\rangle\pm2\langle\phi_f(\tau)\theta_f(\tau')\rangle}.$$

We know that $\langle\phi_f(\tau)\theta_f(\tau')\rangle = 0$. Thus, we have

$$\mathrm{e}^{-2\pi\left\langle(\phi_f(\tau)\pm\theta_f(\tau'))^2\right\rangle} = \mathrm{e}^{-2\pi[\left\langle\phi_f^2(\tau)\right\rangle+\left\langle\theta_f^2(\tau')\right\rangle]}.$$

These two exponentials cancel each other making the whole term zero. Thus, the first- and second-order cumulant expansions can be rewritten as

$$\begin{aligned}&\langle S_{\mathrm{int}}(\phi,\theta)\rangle_f\\ &= b^{-K}\int \mathrm{d}\tau\left(\frac{B}{\pi}\cos(\sqrt{4\pi}\phi_s(\tau))\right)\\ &\quad- b^{-1/K}\int \mathrm{d}\tau\left(\frac{\Delta}{\pi}\cos(\sqrt{4\pi}\theta_s(\tau))\right),\end{aligned} \quad \text{(A.25)}$$

$$\begin{aligned}&-\frac{1}{2}(\langle S_{\mathrm{in}}^2\rangle-\langle S_{\mathrm{int}}\rangle^2)\\ &= \frac{B^2}{4\pi^2}(1-b^{-2K})\int \mathrm{d}\tau(\partial_\tau\phi_s)^2\\ &\quad-\frac{B^2}{2\pi^2}(b^{-4K}-b^{-2K})\int \mathrm{d}\tau\cos[\sqrt{16\pi}\phi_s(\tau)]\\ &\quad+\frac{\Delta^2}{4\pi^2}(1-b^{-2/K})\int \mathrm{d}\tau(\partial_\tau\theta_s)^2\\ &\quad-\frac{\Delta\mu}{\pi^2 v}(1-b^{-1/K})\int \mathrm{d}\tau\cos[\sqrt{4\pi}\theta_s(\tau)].\end{aligned} \quad \text{(A.26)}$$

Now we rescale the first- and second-order cumulant expansions by replacing $\tau = b\tau'$, $\omega = \omega'/b$, $\phi_s(\tau) = \phi'(\tau')$ and $\phi(\omega) = b\phi'(\omega')$.

$$\begin{aligned}\langle S_{\mathrm{int}}(\phi,\theta)\rangle_f &= b^{2-K}\int \mathrm{d}\tau'\left(\frac{B}{\pi}\cos(\sqrt{4\pi}\phi'(\tau'))\right)\\ &\quad-b^{2-\frac{1}{K}}\int \mathrm{d}\tau'\left(\frac{\Delta}{\pi}\cos(\sqrt{4\pi}\theta'(\tau'))\right),\end{aligned} \quad \text{(A.27)}$$

$$\begin{aligned}&-\frac{1}{2}(\langle S_{\mathrm{int}}^2\rangle-\langle S_{\mathrm{int}}\rangle^2)\\ &= \frac{B^2}{4\pi^2}(b^2-b^{2-2K})\int \mathrm{d}\tau'(\partial_{\tau'}\phi')^2\\ &\quad-\frac{B^2}{2\pi^2}(b^{2-4K}-b^{2-2K})\int \mathrm{d}\tau'\cos[\sqrt{16\pi}\phi'(\tau')]\\ &\quad+\frac{\Delta^2}{4\pi^2}(b^2-b^{2-\frac{2}{K}})\int \mathrm{d}\tau'(\partial_{\tau'}\theta')^2\\ &\quad-\frac{\Delta\mu}{\pi^2 v}(b^2-b^{2-\frac{1}{K}})\int \mathrm{d}\tau'\cos[\sqrt{4\pi}\theta'(\tau')].\end{aligned} \quad \text{(A.28)}$$

Comparison of B terms gives

$$B' = Bb^{2-K}.$$

We put $b = \mathrm{e}^{\mathrm{d}l}$ and expand the exponential up to second term, i.e., $\mathrm{e}^{\mathrm{d}l} = 1+\mathrm{d}l$. Then,

$$\begin{aligned}B' &= B[1+(2-K)\mathrm{d}l],\\ &= B+(2-K)B\mathrm{d}l.\end{aligned}$$

We define $B' - B = \mathrm{d}B$. Thus, we have

$$\boxed{\frac{\mathrm{d}B}{\mathrm{d}l} = (2-K)B}. \tag{A.29}$$

Comparison of Δ terms gives

$$\begin{aligned}\Delta' &= \Delta(b^{2-\frac{1}{K}}) - \frac{\Delta\mu}{\pi v}(b^2 - b^{2-\frac{1}{K}}) \\ &= \Delta(\mathrm{e}^{(2-\frac{1}{K})\mathrm{d}l}) - \frac{\Delta\mu}{\pi v}(\mathrm{e}^{2\mathrm{d}l} - \mathrm{e}^{(2-\frac{1}{K})\mathrm{d}l}) \\ &= \Delta + \left(2 - \frac{1}{K}\right)\Delta\mathrm{d}l - \frac{\Delta\mu}{\pi v K}\mathrm{d}l.\end{aligned}$$

Thus, the equation in differential form is

$$\boxed{\frac{\mathrm{d}\Delta}{\mathrm{d}l} = \left[2 - \frac{1}{K}\left(1 + \frac{\mu}{v\pi}\right)\right]}. \tag{A.30}$$

Comparison of K terms for ϕ field gives

$$\begin{aligned}\frac{1}{K'} &= \frac{1}{K}\left[1 + \frac{B^2}{4\pi^2}(b^2 - b^{2-2K})\right] \\ &= \frac{1}{K}\left[1 + \frac{B^2}{4\pi^2}(\mathrm{e}^{2dl} - \mathrm{e}^{(2-2K)\mathrm{d}l})\right] \\ &= \frac{1}{K} + \frac{B^2}{2\pi^2}\mathrm{d}l.\end{aligned}$$

Differential form can obtained as

$$\frac{\mathrm{d}}{\mathrm{d}l}\left(\frac{1}{K}\right) = \frac{B^2}{2\pi^2}.$$

$$\frac{\mathrm{d}K}{\mathrm{d}l} = -\frac{B^2K^2}{2\pi^2}. \tag{A.31}$$

Similarly, for θ field,

$$\begin{aligned}K' &= K + \frac{\Delta^2 K}{4\pi^2}(b^2 - b^{2-2/K}) \\ &= K + \frac{\Delta^2 K}{4\pi^2}(\mathrm{e}^{2dl} - \mathrm{e}^{(2-\frac{2}{K})dl}) \\ &= K + \frac{\Delta^2}{2\pi^2}\mathrm{d}l.\end{aligned}$$

The differential form is

$$\frac{\mathrm{d}K}{\mathrm{d}l} = \frac{\Delta^2}{2\pi^2}. \tag{A.32}$$

Thus, the complete form of the differential equation for K is

$$\boxed{\frac{\mathrm{d}K}{\mathrm{d}l} = \frac{1}{2\pi^2}(\Delta^2 - B^2K^2)}. \tag{A.33}$$

Thus, we obtain the whole set of RG equations,

$$\begin{aligned}\frac{\mathrm{d}B}{\mathrm{d}l} &= (2-K)B. \\ \frac{\mathrm{d}\Delta}{\mathrm{d}l} &= \left[2 - \frac{1}{K}\left(1 + \frac{\mu}{v\pi}\right)\right]. \\ \frac{\mathrm{d}K}{\mathrm{d}l} &= \frac{1}{2\pi^2}(\Delta^2 - B^2K^2).\end{aligned} \tag{A.34}$$

References

[1] P Coleman, *Quantum many body physics* (Cambridge University Press, United Kingdom, 2015)
[2] P W Anderson, *Science* **1777**, 393 (1972)
[3] P W Anderson, *Basic notion of condensed matter physics* (Benjamin Cummings, 1984)
[4] M Z Hasan and C L Kane, *Rev. Mod. Phys.* **82**, 3045 (2010)
[5] J E Moore, *Nature* **464**, 194 (2010)
[6] S Barik, A Karasahin, C Flower, T Cai, H Miyake, W DeGottardi, M Hafezi and E Waks, *Science* **359**, 666 (2018)
[7] S D Sarma, M Freedman and C Nayak, *Npj Quantum Inf.* **1**, 1 (2015)
[8] K V Klitzing, G Dorda and M Pepper, *Phys. Rev. Lett.* **45**, 494 (1980)
[9] D J Thouless, M Kohmoto, M P Nightingale and M den Nijs, *Phys. Rev. Lett.* **49**, 405 (1982)
[10] B A Bernevig and S C Zhang, *Phys. Rev. Lett.* **96**, 106802 (2006)
[11] B A Bernevig, T L Hughes and S C Zhang, *Science* **314**, 1757 (2006)
[12] M König, S Wiedmann, C Brüne, A Roth, H Buhmann, L W Molenkamp, X L Qi and S C Zhang, *Science* **318**, 766 (2007)
[13] C Wu, B A Bernevig and S C Zhang, *Phys. Rev. Lett.* **96**, 106401 (2006)
[14] T Li, P Wang, H Fu, L Du, K A Schreiber, X Mu, X Liu, G Sullivan, G A Csathy, X Lin and R R Du, *Phys. Rev. Lett.* **115**, 136804 (2015)
[15] E Sela, A Altland and A Rosch, *Phys. Rev. B* **84**, 085114 (2011)
[16] S Sarkar, *Sci. Rep.* **6**, 30569 (2016)
[17] Duncan Haldane (Nobel Prize in Physics 2016), Distinguished lecture on 11 January 2019 at ICTS, India
[18] A Altland and B D Simons, *Condensed matter field theory* (Cambridge University Press, 2010)
[19] E Fradkin, *Field theories of condensed matter physics* (Cambridge University Press, 2013)
[20] E C Marino, *Quantum field theory approach to condensed matter physics* (Cambridge University Press, 2017)
[21] R Shankar, *Quantum field theory and condensed matter: An introduction* (Cambridge University Press, 2017)

[22] V L Berezinskii, *Sov. Phys. JETP* **32**, 493 (1971)
[23] J M Kosterlitz and D J Thouless, *J. Phys. C* **6**, 1181 (1973)
[24] G Ortiz, E Cobanera and Z Nussinov, Berezinskii–Kosterlitz–Thouless transition through the eyes of duality, in: *40 Years of Berezinskii–Kosterlitz–Thouless Theory* (World Scientific, 2013) pp. 93–134
[25] C L Kane and E J Mele, *Phys. Rev. Lett*. **95**, 146802 (2005)
[26] F Pollmann, E Berg, A M Turner and M Oshikawa, *Phys. Rev. B* **85**, 075125 (2012)
[27] S Gangadharaiah, B Braunecker, P Simon and D Loss, *Phys. Rev. Lett.* **107**, 036801 (2011)
[28] K C Nowack, E m Spanton, M Baenninger, M König, J R Kirtley, B Kalisky, C Ames, P Leubner, C Brüne, H Buhmann and L W Molenkamp, *Nature Mater*. **12**, 787 (2013)
[29] E M Spanton, K C Nowack, L Du, G Sullivan, R R Du and K A Moler, *Phys. Rev. Lett.* **113**, 026804 (2014)
[30] C W J Beenakker, *Annu. Rev. Condens. Matter Phys*. **4**, 113 (2013)
[31] D Hsieh, D Qian, L Wray, Y Xia, Y S Hor, R J Cava and M Z Hasan, *Nature* **452**, 970 (2008)